Evapotranspiration estimation considering anthropogenic heat based on remote sensing in urban area

Article

Accepted Version

Evapotranspiration estimation considering anthropogenic heat based on remote sensing in urban area

CONG ZhenTao[1, 2*], SHEN QiNing[1], ZHOU Lin[1], SUN Ting[1], LIU JiaHong[3]

[1] *State Key Laboratory of Hydro-Science and Engineering, Department of Hydraulic Engineering, Tsinghua University, Beijing 100084, China*
[2] *Sanjiangyuan Collaborative Innovation Center, Tsinghua University, Beijing 100084, China*
[3] *China Institute of Water Resources and Hydropower Research, Beijing 100038, China*

* Corresponding Author (email: congzht@tsinghua.edu.cn)

Abstract

Urbanization influences hydrologic cycle significantly on local, regional even global scale. With urbanization the water resources demand for dense population sharpened, thus it is a great challenge to ensure water supply for some metropolises such as Beijing. Urban area is traditionally considered as the area with lower evapotranspiration (ET) on account of the impervious surface and the lower wind speed. For most remote sensing models, the ET, defined as latent heat in energy budget, is estimated as the difference between net radiation and sensible heat. The sensible heat is generally higher in urban area due to the high surface temperature caused by heat island, therefore the latent heat (i.e. the ET) in urban area is lower than that in other region. We estimated water consumption from 2003 to 2012 in Beijing based on water balance method and found that the annual mean ET in urban area was about 654 mm. However, using Surface Energy Balance System (SEBS) model, the annual mean ET in urban area was only 348 mm. We attributed this inconsistence to the impact of anthropogenic heat and quantified this impact on the basis of the night-light maps. Therefore, a new model SEBS-Urban, coupling SEBS model and anthropogenic heat was developed to estimate the ET in urban area. The ET in urban area of Beijing estimated by SEBS-Urban showed a good agreement with the ET from water balance method. The findings from this study highlighted that anthropogenic heat should be included in the surface energy budget for a highly urbanized area.

Keywords:

Urban; Evapotranspiration; SEBS; Remote sensing; Anthropogenic heat

1. **Introduction**

Urbanization is progressing at a rapid rate on a global scale. Over half of population now lives in urban area, and by 2050 that fraction is expected to exceed 70% (Bratman et al., 2015; Heilig, 2012). Natural terrains are continuously converted to urban landscapes to meet the ever-increasing demand of the expanding urban population (Yang et al., 2015). The surface and atmospheric conditions in urban areas are modified, resulting in large variation of regional hydroclimate and energy balance (Oke, 2002; Tam et al., 2015; Yang et al., 2016; Zhang et al., 2009; Zhong et al., 2015). In addition, human activities make cities more vulnerable to a number of water resource problems (Bai and Imura, 2001; Iglesias et al., 2007; Jiang, 2009; Paul and Meyer, 2008). Therefore, further understanding of water cycle and energy balance in urban areas is necessary for future water resources planning.

Evapotranspiration (ET) is a combination of two processes: evaporation of liquid water from various surfaces and transpiration from the plants through stomata (Allen et al., 1998). It is a major component of water cycle and plays a vital role in surface energy balance system. In urban areas, ET research is central to green spaces irrigation, water consumption monitoring as well as the mechanism by which rainfall retention capacity is recovered between storm events. Common ET estimation procedures were developed for agricultural applications, however, researches on ET remained limited in urban areas (DiGiovanni et al., 2012; Grimmond and Oke, 1991; Zheng, 2012). In that regard, reliable estimation of urban ET is of particular importance for development of urban hydrology and water resource management.

A number of methods have been developed to estimate ET, including water balance method (Alley, 1984; Granier et al., 1999; Long and Singh, 2010; Palmroth et al., 2010; Senay et al., 2011; Xu and Singh, 2005), meteorological method (Alexandris et al., 2008; McMahon et al., 2013; Penman, 1948; Priestley and Taylor, 1972; Sumner and Jacobs, 2005) and remotely-sensed energy balance model (Allen et al., 2007; Bastiaanssen et al., 1998; Roerink et al., 2000; Su, 2002). For the acquisition of free information at all scales, remote sensing data has been extensively applied in numerous fields. The most popular remotely-sensed models include the Surface Energy Balance System (SEBS) (Su, 2002), the Surface Energy Balance Algorithm for Land (SEBAL) (Bastiaanssen et al., 1998), and the Mapping Evapotranspiration at High Resolution with Internalized Calibration (METRIC) (Allen et al., 2007), which have been widely used in ET estimation from regional to continental scales.

In ET estimation, remote sensing based methods provide a feasible alternative to the spatiotemporal characteristics of ET at different scales, which have advantages over the other approaches. In traditional remotely sensed models, the anthropogenic heat and net advection are negligible in energy balance equation. However, in cities anthropogenic heat from human metabolism, vehicles and building heat emissions is a significant contribution to the surface energy budget (Allen et al., 2011; McCarthy et al., 2010; Sailor, 2011). Anthropogenic heat is 0.028 W m^{-2} on global average, while localized estimation ranges from tens to hundreds of W m^{-2} and even as high as 1590 W m^{-2} for the extreme business district of Tokyo (Flanner, 2009; Ichinose et al., 1999; Kłysik, 1996; Pigeon et al., 2007; Sailor and Lu, 2004). Therefore, the impacts of anthropogenic heat are usually considerable and should be included in the surface energy budget for a highly urbanized area.

In this study, we hypothesize that ET was equal to the water consumption in the study area. The objectives of this study were (1) to estimate annual ET in Beijing based on water balance model and the original SEBS model; (2) to consider the influence of

anthropogenic heat on ET in Beijing by a modified SEBS model (will be called as SEBS-Urban in the following); (3) to discuss the results and uncertainties in ET estimation.

This paper is organized as follows. The study area and data are given in the Section 2; Section 3 is the description of methods used (water balance method, SEBS model and SEBS-Urban model); the results and discussions are shown in Section 4; the conclusions are presented in Section 5.

2. Study area and data

2.1 Study area

Beijing (115°25'~117°30'E，39°26'~41°04'N), the capital of China, is located at North China Plain with a coverage of about 16410 km^2 (see **Figure 1a**). The region has a typical temperate and monsoonal climate, with an annual mean rainfall of 576 mm and an annual mean temperature of about 12.5 ℃ from 1961 to 2010 (Li and Yang, 2015; You et al., 2012). Beijing is the political and cultural center of China, with a history of over 3000 years and a permanent population of more than 20 million (Beijing Municipal Bureau of Statistics, 2012, website: http://www.bjstats.gov.cn/English/MR/Population/ 201603/t20160303_337912.html). However, it is one of the most water-deficient metropolises in the world. The per capita water resources available is about 150 m³ in Beijing in 2012, which is far below the international minimum standard of 1000 m³ per capita defined by the United Nations (Wang and Wang, 2005). There are many water regulation projects in the city and the Miyun reservoir is the primary project to ensure potable water for Beijing.

Woodland, farmland and urban land are the major land use types in Beijing (see **Figure 1b**) and the geography of the city is characterized by alluvial plains in the southeast and mountains in the north and west (see **Figure 1c**). In this study, Beijing was divided into a mountain area of 10174 km^2 and a plain area of 6236 km^2 in accordance with elevation and surface heterogeneity. Based on the land use data, the plain area was further subdivided into urban area and suburban area, which are changing over time with average of 1154 km^2 and 5082 km^2, respectively (see **Figure 1a**).

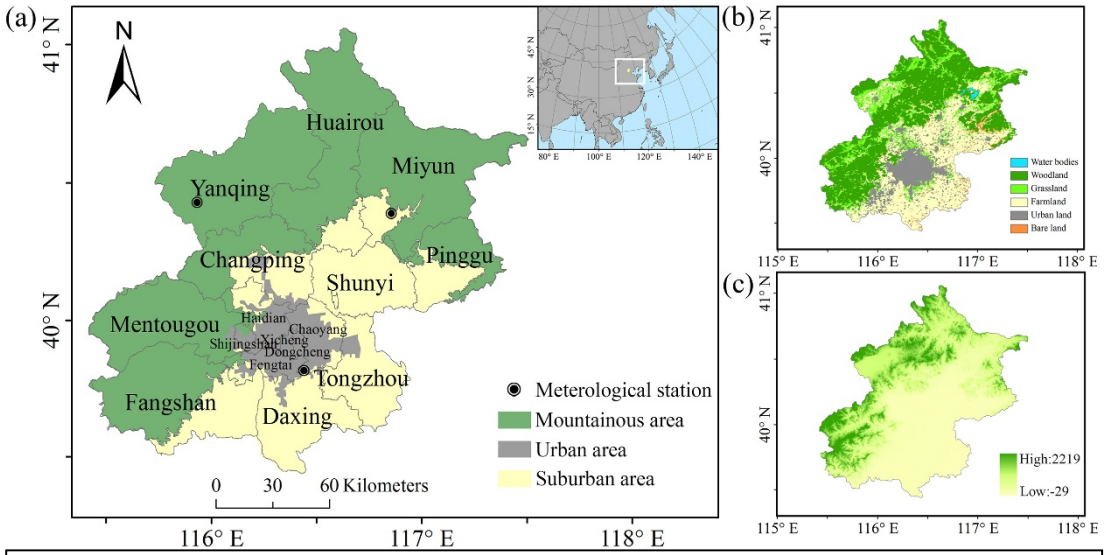

Figure 1. Information of the study area: (a) the location and the subareas of Beijing; (b) the land use map; (c) the elevation map.

2.2 Data

2.2.1 Data for water balance method

The data used in water balance method were mainly collected from the Beijing Water Resources Bulletin (Beijing Water Authority, website: http://www.bjwater.gov.cn/pub/bjwater/zfgk/tjxx/index_1.html) and Beijing Statistical Yearbook (Beijing Municipal Bureau of Statistics, website: http://www.bjstats.gov.cn/tjsj/). Due to the limited resources, the study concentrated on the period from 2003 to 2012. In addition, the divisional precipitation was estimated based on the combination of meteorological stations and local precipitation contour maps.

2.2.2 Data for remote sensing models

Remote sensing products are the key inputs to SEBS model. The information of the input data are listed in **Table 1**. In this study, emissivity, LAI, NDVI, LST and land use data were derived from MODIS standard products (website: http://reverb.echo.nasa.gov/). Land surface albedo was retrieved using the algorithm proposed by Liang (2001). NDVI values were scaled to fractional vegetation cover as follow (Gillies and Carlson, 1995):

$$f_c = \frac{NDVI - NDVI_{\min}}{NDVI_{\max} - NDVI_{\min}} \quad (1)$$

where f_c is fractional vegetation cover, $NDVI_{\min}$ is the minimum $NDVI$, which can be estimated as the averaged $NDVI$ for bare soil, $NDVI_{\max}$ is the maximum $NDVI$, which can be estimated as the averaged $NDVI$ for forest.

Meteorological elements including air temperature, pressure, specific humidity, wind speed, downward shortwave radiation and downward longwave radiation were collected from China Meteorological Forcing Dataset (He and Yang, 2011). The evaluation of anthropogenic heat was based on the remote sensing nighttime lights data, a product of DMSP/OLS (website: http://ngdc.noaa.gov/eog/). All the information was interpolated into daily maps at 500 m resolution, using the linear interpolation method.

The quality of remote sensing image is affected by weather condition. In this study, only the cloud-free days with high-quality images of MODIS were selected for the analysis. The number of selected days in the study period are listed in **Table 2**.

Table 1. Information of the remote sensing data used in SEBS model.

Data	Source	Spatial resolution	Temporal resolution	Time period
Emissivity	MOD11A1	1km	Daily	2003-2012
LAI	MOD15A2	1km	8 days	2003-2012
NDVI	MOD13A2	1km	16 days	2003-2012
LST	MOD11A1	1km	Daily	2003-2012
Land use	MCD12Q1	500m	yearly	2003-2012
Albedo	MOD09GA	500m	Daily	2003-2012
Air temperature	China Meteorological Forcing Dataset	0.1° × 0.1°	3 hr	2003-2012
Pressure	China Meteorological Forcing Dataset	0.1° × 0.1°	3 hr	2003-2012

Specific humidity	China Meteorological Forcing Dataset	$0.1° \times 0.1°$	3 hr	2003-2012
Wind speed	China Meteorological Forcing Dataset	$0.1° \times 0.1°$	3 hr	2003-2012
Downward shortwave radiation	China Meteorological Forcing Dataset	$0.1° \times 0.1°$	3 hr	2003-2012
Downward longwave radiation	China Meteorological Forcing Dataset	$0.1° \times 0.1°$	3 hr	2003-2012
Nighttime lights data	DMSP/OLS	1km	yearly	2003-2012

Table 2. The number of selected days in the study period (2003-2012).

Year	2003	2004	2005	2006	2007	2008	2009	2010	2011	2012
Number of days	60	64	91	57	82	72	90	77	64	80

3. Methodology

3.1 Water balance method

It was assumed that ET was equal to the water consumption in the study area. Based on the water balance equation, the annual ET can be estimated as follow:

$$ET = P + 10^5 \left(S_i - S_o + G_i - G_o - \Delta S - \Delta G \right) / A \quad (2)$$

$$ET_m = P_m + 10^5 \left(S_{mi} - S_{mo} + G_{mi} - G_{mo} - \Delta S_m - \Delta G_m \right) / A_m \quad (3)$$

$$ET_p = P_p + 10^5 \left(S_{pi} - S_{po} + G_{pi} - G_{po} - \Delta S_p - \Delta G_p \right) / A_p \quad (4)$$

$$ET_u = P_u + 10^5 \left(S_{ui} - S_{uo} + G_{ui} - G_{uo} - \Delta S_u - \Delta G_u \right) / A_u \quad (5)$$

$$ET_s = P_s + 10^5 \left(S_{si} - S_{so} + G_{si} - G_{so} - \Delta S_s - \Delta G_s \right) / A_s \quad (6)$$

Eq. (2) to Eq. (6) are for the entire area, mountainous area, plain area, urban area and suburb area, respectively, where ET is the annual evapotranspiration, mm; P is the annual precipitation, mm; S_i is the annual surface inflow, i.e. the supply from runoff and South-North Water Transfer Project, 10^8 m^3; S_o is the annual surface outflow, 10^8 m^3; G_i is the annual groundwater input, 10^8 m^3; G_o is the annual groundwater outflow, 10^8 m^3, and it was assumed that G_o equaled G_i in this study; ΔS is the variation in surface water storage, 10^8 m^3, estimating from change in reservoir storage; ΔG is the variation in groundwater storage, 10^8 m^3; A is the corresponding area, km^2.

Figure 2 shows the water balance of subareas in Beijing. Note that in mountainous area, S_{mi} was estimated as the annual runoff supply; S_{mo} was calculated as surface water resources in mountainous area; G_{mi} was equal to G_i; G_{mo} was regarded as water supply from mountainous area to plain area; ΔG_m was generally neglected due to few extraction of groundwater and the self-adjustment of ecosystem; and ΔS_m was equal to ΔS. When it comes to plain area, S_{pi} was considered as the sum of S_{mo} and annual supply from South–North Water Transfer Project; S_{po}, G_{pi}, G_{po} and ΔG_p were equal to S_o, G_{mo}, G_o, and ΔG, respectively; and ΔS_p was neglected considering that there were few large scale reservoirs in plain area. As for urban area, S_{ui} was estimated as the difference between water supply (includes industrial, domestic and ecological water use) and underground water exploited in urban area; S_{uo} was considered as urban drainage; G_{ui} was estimated according to the underground supply from mountainous area; G_{uo} was neglected due to the intensive extraction of underground water in urban area; ΔG_u was calculated as $\Delta G_u = \Delta G \times A_u / A_p$; and ΔS_u was neglected. With regard to suburb area, S_{si}, S_{so}, G_{si}, G_{so} ΔG_s and ΔS_s were calculated as the differences between the corresponding items in plain

area and urban area.

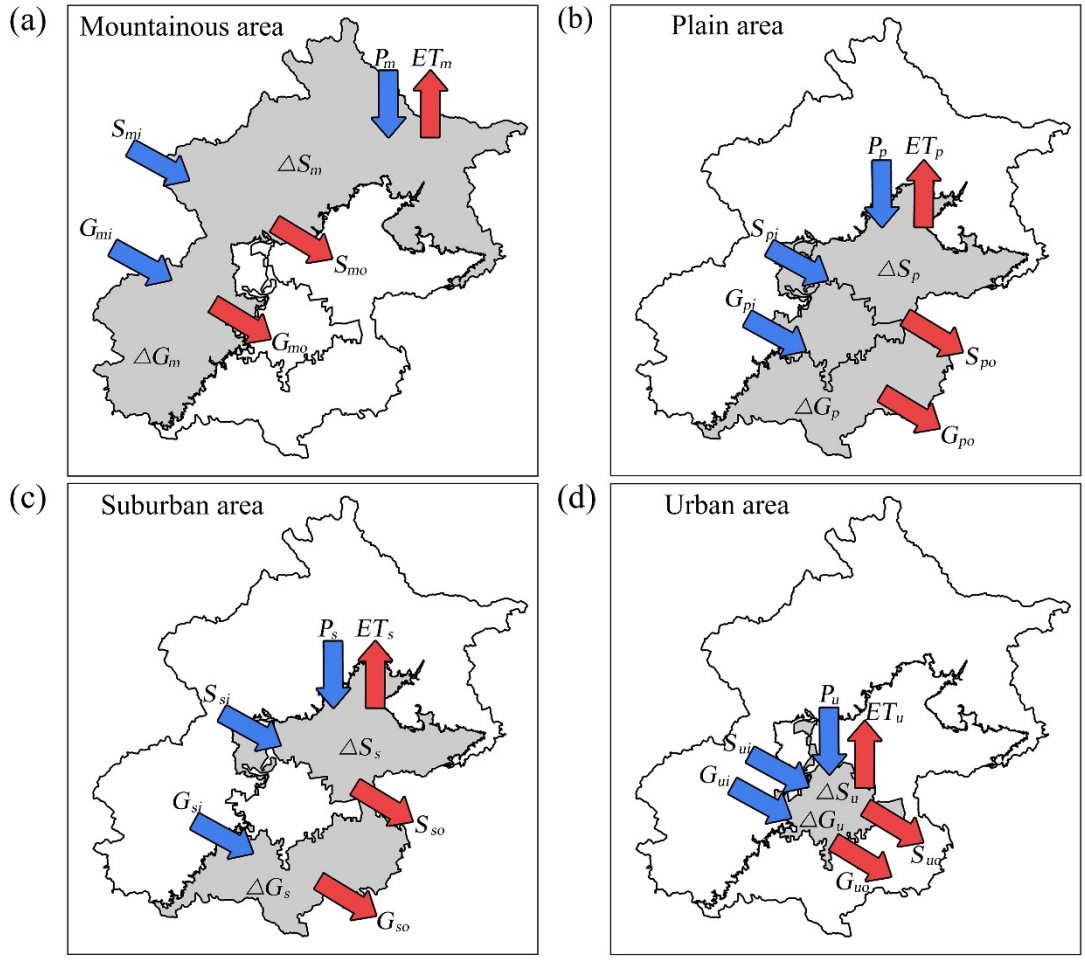

Figure 2. Water balance of subareas in Beijing. Blue arrows and red arrows represent water input and output, respectively.

3.2 Surface Energy Balance System (SEBS) model

The Surface Energy Balance System (SEBS) was developed by Su (2002) for the estimation of turbulent heat fluxes and the daily evapotranspiration using remote sensing data. Only the main SEBS equations and concepts are presented in this paper, further details were given by Su et al. (2001) and Su (2002). The SEBS algorithm is based on the energy balance equation expressed as:

$$R_n = G_0 + H + \lambda ET \tag{7}$$

where R_n is net radiation, W m^{-2}; G_0 is soil heat flux, W m^{-2}; H is sensible heat flux, W m^{-2} and λET is the latent heat flux, W m^{-2} (λ is the latent heat of vapourization and ET is evapotranspiration). R_n is calculated by:

$$R_n = (1-\alpha)\cdot R_{swd} + \varepsilon \cdot R_{lwd} - \varepsilon \cdot \sigma \cdot T_0^4 \tag{8}$$

where α is albedo, R_{swd} is downward shortwave radiation, W m^{-2}; R_{lwd} is downward longwave radiation, W m^{-2}; ε is emissivity; σ is the Stefan-Boltzmann constant, W m^{-2} K^{-4}; and T_0 is surface temperature, K.

The soil heat flux is calculated taking into account fractional vegetation cover:

$$G_0 = R_n \cdot \left[\Gamma_c + (1-f_c)\cdot(\Gamma_s - \Gamma_c)\right] \tag{9}$$

where f_c is fractional vegetation cover; $\Gamma_c = 0.05$ (dimensionless) for full vegetation cover and $\Gamma_s = 0.315$ (dimensionless) for bare soil. An interpolation is then performed between the two limiting cases based on f_c.

For deriving the sensible and latent heat flux, the similarity theory was used. In SEBS model, distinction were made between the Atmospheric Boundary Layer (ABL) and the Atmospheric Surface Layer (ASL). Since the field measurements were performed in ASL, the Monin-Obukhov Similarity (MOS) functions by Brutsaert (1999) were used. For stable conditions in ASL, the equations proposed by Beljaars and Holtslag (1991) and Van den Hurk and Holtslag (1997) were used, while in ABL the functions proposed by Brutsaert (1982) were used. The MOS expressions are not presented in this paper.

The roughness height for momentum transfer and roughness height for heat transfer were calculated taking into account the canopy height h and reference height z_{ref}. The equations were given by Su (2001; 2002) based on surface layer similarity theory (Brutsaert, 1982):

$$z_{0m} = h \cdot (1 - d_0 / h) \cdot e^{-ku(h)/u_*} \tag{10}$$

$$d_0 / h = 1 - (1 - e^{-2n_{ec}}) / 2n_{ec} \tag{11}$$

$$n_{ec} = C_d \cdot LAI / (2u_*^2 / u(h)^2) \tag{12}$$

$$u(h) = u_{ref} \frac{\ln(h - d / z_{0m})}{\ln(z_{ref} - d / z_{0m})} \tag{13}$$

$$z_{0h} = z_{0m} / e^{kB^{-1}} \tag{14}$$

where z_{0m} is the roughness height for momentum transfer; h is the canopy height; d_0 is the displacement height; k is the von Karman constant with a numeric value of 0.4; $u(h)$ is the horizontal wind speed at the canopy top; u_* is the friction velocity; n_{ec} is the within-canopy wind speed profile extinction; C_d is the drag coefficient taken as 0.2; LAI is the leaf area index; u_{ref} is the reference wind speed; z_{ref} is the reference height; and B^{-1} is the inverse Stanton number. See Su (2002) for more details.

In this study, the essential parameter h was estimated in accordance with different land use types from MODIS. The land use types were reclassified into 10 types based on the definition given by International Geosphere-Biosphere Programme (IGBP) and the corresponding values of canopy height were obtained from relative researches in Beijing (see **Table 3**).

Table 3. The values of the parameter h in this study.

Code in MODIS	Class name	Recode	Rename	h	Reference
0	Water Bodies	0	Water Bodies	0.0001	---
1	Evergreen Needleleaf Forest	1	Evergreen Forest	10~12	(Che, 2008; Zhang et al., 2014; Zhang, 2011)
3	Deciduous Needleleaf Forest	2	Deciduous Forest	10~12	(Che, 2008; Zhang et al., 2014; Zhang, 2011)
4	Deciduous Broadleaf Forest	2	Deciduous Forest	10~12	(Che, 2008; Zhang et al., 2014; Zhang, 2011)
5	Mixed Forest	3	Mixed Forest	10~12	(Che, 2008; Zhang et al., 2014; Zhang, 2011)

6	Closed Shrublands	4	Shrublands	1.2~2.5	(Che, 2008; Du and Xing, 2009)
7	Open Shrublands	4	Shrublands	1.2~2.5	(Che, 2008; Du and Xing, 2009)
8	Woody Savannas	5	Grasslands	0.005~0.03	(Xu et al., 2009)
9	Savannas	5	Grasslands	0.005~0.03	(Xu et al., 2009)
10	Grasslands	5	Grasslands	0.005~0.03	(Xu et al., 2009)
11	Permanent Wetlands	6	Wetlands	0.0001	---
12	Croplands	7	Croplands	0.003~1	(Song et al., 2009)
13	Urban and Built-Up	8	Urban	20	(He et al., 2001; Shi et al., 2015)
14	Cropland/Natural Vegetation Mosaic	9	Bare land	0.0005	---
15	Snow and Ice	9	Bare land	0.0005	---
16	Barren or Sparsely Vegetated	9	Bare land	0.0005	---

The value of H was then determined by considering the dry-limit and wet-limit conditions. Under dry-limit condition (soil moisture at limiting cases), the latent heat becomes zero while the sensible heat flux is at its maximum value. By definition, from Eq. (7), it follows that:

$$\lambda ET_{dry} = R_n - G_0 - H_{dry} \equiv 0 \quad \text{or} \quad H_{dry} = R_n - G_0 \tag{15}$$

Under wet-limit condition (energy at limiting cases), ET occurs at the potential rate, while sensible heat flux takes its minimum value, which therefore follows:

$$\lambda ET_{wet} = R_n - G_0 - H_{wet} \quad \text{or} \quad H_{wet} = R_n - G_0 - \lambda ET_{wet} \tag{16}$$

Then the evaporative fraction, Λ was expressed as:

$$\Lambda = \frac{\lambda ET}{R_n - G_0} \tag{17}$$

By inverting Eq. (12), the latent heat can be calculated as:

$$\lambda E = \Lambda \cdot (R_n - G_0) \tag{18}$$

Actual ET converted to water depth in mm per time unit was then calculated by $ET = \lambda ET / (\lambda \cdot \rho_w)$, where ρ_w is the density of water kg m^{-3} (Jia et al., 2009).

Note that satellite images provide for the instantaneous observation in time, therefore, daily ET was derived by assuming that the evaporative fraction remain constant throughout the day (Jia et al., 2009; Sugita and Brutsaert, 1991). The daily ET was then given by:

$$\begin{aligned} ET_{daily} &= \sum_{i=0}^{24} \left[\Lambda \cdot \frac{R_n - G}{\lambda \rho_w} \right] \\ &= 24(\mathrm{h}) \cdot 3600(\mathrm{s}) \cdot \left[\Lambda \cdot \frac{R_{ndaily} - G_{daily}}{\lambda \rho_w} \right] \\ &= 8.67 \times 10^7 \cdot \left[\Lambda \cdot \frac{R_{ndaily} - G_{daily}}{\lambda \rho_w} \right] \end{aligned} \tag{19}$$

where ET_{daily} is the daily evapotranspiration, mm; R_{ndaily} is the daily mean net

radiation, W m^{-2};; G_{daily} is the daily mean soil surface heat flux, W m^{-2}; ρ_w is the density of water, kg m^{-3}; λ is the latent heat of vapourization taken as 2.45×10^6 J kg^{-1}.

Since the ET was estimated from discrete remote sensing images, to produce time series of ET, the crop coefficient method proposed by Allen (2000) was used for reference in this study. Researches indicate that crop coefficient method is generally sufficient to estimate time series of ET, also on a monthly basis (Morse et al., 2000; Allen et al., 2001; Allen et al., 2007). Thus this method is considered valid for extending ET series in Beijing, where the image intervals are no more than two weeks.

The crop coefficient is basically the ratio of actual ET to the reference evapotranspiration (ET_0). The crop coefficient method interpolated the crop coefficients derived from remotely sensed actual ET and corresponding ET_0 for the days of image available. Then combining the interpolated crop coefficient with ET_0, actual ET for days without good quality images could be inferred, which was formulated as:

$$ET_{period} = \sum_{i=b}^{f}\left[\frac{1}{2}\left(\frac{ET_b}{ET_{0b}}+\frac{ET_f}{ET_{0f}}\right)\left(ET_{0i}\right)\right] \tag{20}$$

where ET_{period} represents the accumulated actual ET for a period with beginning day *b* and ending day *f*, which are cloud-free days; ET_b *and* ET_f are the actual ET derived from the beginning day and ending day, respectively; ET_{0b} and ET_{0f} are the corresponding reference ET for the beginning day and ending day, respectively; and ET_{0i} is the reference ET for day *i*. In this study, the reference ET was calculated using FAO-Penman-Monteith equation (Allen et al., 1998).

3.3 SEBS-Urban model

In traditional remote sensing-based models, the anthropogenic heat and net advection are neglected in energy balance equation. However, in metropolis with intensive human activities, anthropogenic heat would contribute significantly to the surface energy budget (Allen et al., 2011; McCarthy et al., 2010; Sailor, 2011). High anthropogenic heat is generally observed in Beijing and in the densely built-up areas the hourly maximum value even as high as 474.3 W m^{-2}. (Nie et al., 2014; Tong et al., 2004). In this section, anthropogenic heat was quantified to estimate ET in Beijing by a modified SEBS model. Therefore, the energy balance equation was given as:

$$R_n + Q_f = G_0 + H + \lambda ET \tag{21}$$

where R_n is net radiation, W m^{-2}; Q_f is anthropogenic heat, W m^{-2}; G_0 is soil heat flux, W m^{-2}; H is sensible heat flux, W m^{-2} and λET is the latent heat flux, W m^{-2}.

The evaluation of anthropogenic heat was based on the remote sensing product of DMSP/OLS, which provide annual averaged nighttime lights maps with numeric values range from 0 to 63. In this study, the threshold value was defined as 52 for separating the anthropogenic heat-impacted areas from the anthropogenic heat-free areas (Shu et al., 2011). The values of anthropogenic heat were set as a range from 50 W m^{-2} to 75 W m^{-2} for summer and winter, and 30 W m^{-2} to 50 W m^{-2} for spring and autumn, on the basis of researches conducted by Nie et al. (2014) and Tong et al. (2004). Then the corresponding light intensity limits were 52 and 63 and the internal values were produced by linear interpolation. Therefore, the value of anthropogenic heat was given as:

$$Q_{f1} = Q_{fl1} + (I - I_{\min})\cdot\frac{Q_{fu1} - Q_{fl1}}{I_{\max} - I_{\min}} \tag{22}$$

$$Q_{f2} = Q_{fl2} + (I - I_{\min}) \cdot \frac{Q_{fu2} - Q_{fl2}}{I_{\max} - I_{\min}} \quad (23)$$

Eq. (22) is for summer and winter, where Q_{fl} is the anthropogenic heat, W m^{-2}; Q_{fl1} (50 W m^{-2}) and Q_{fu1} (75 W m^{-2}) are the lower limit and upper limit of anthropogenic heat, respectively; I is the numeric value of light intensity; I_{max} is the maximum light intensity with a value of 63; I_{min} is the minimum light intensity set as 52, i.e. the threshold value for identifying the anthropogenic heat-impacted areas.

Eq. (23) is for spring and autumn, where Q_{fl2} (30 W m^{-2}) and Q_{fu2} (50 W m^{-2}) are the lower limit and upper limit of anthropogenic heat, respectively; and the other items are set ibid.

4. Results and discussions

4.1 ET estimated by water balance method

ET estimation of each subarea based on water balance method from 2003 to 2012 are listed in **Table 4**. It can be seen that the average ET in Beijing from 2003 to 2012 was 517 mm, which was roughly equivalent to average precipitation of 523 mm. This indicates that Beijing made little contribution to the water resources of Hai River Basin. It should be noted that averaged annual ET in urban area was the highest among all subareas (654 mm), while the lowest in mountainous area (472 mm). **Figure 3a** and **Figure 3b** shows the averaged ET and water input/output over the decade in entire Beijing and urban area, respectively. According to **Figure 3**, precipitation made up most of ET in entire Beijing at a long-term scale, however, as for urban area surface inflow and precipitation both contributed greatly to ET. **Figure 4** illustrates the time series of ET estimated by water balance method in subareas of Beijing from 2003 to 2012. It can also be observed that ET in urban area was generally higher than other areas. Additionally, relative smooth changes in ET were observed in plain area and suburban area, while a dramatic variation was shown in mountainous area. This may be attributed to the significant fluctuation of rainfall received in mountain region.

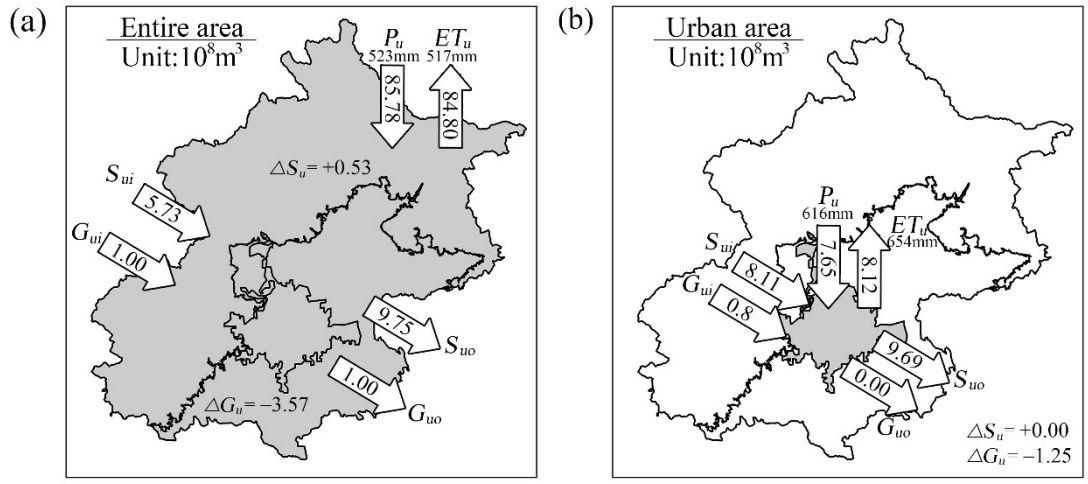

Figure 3. Averaged annual precipitation and ET in entire Beijing and urban area over 2003 to 2012.

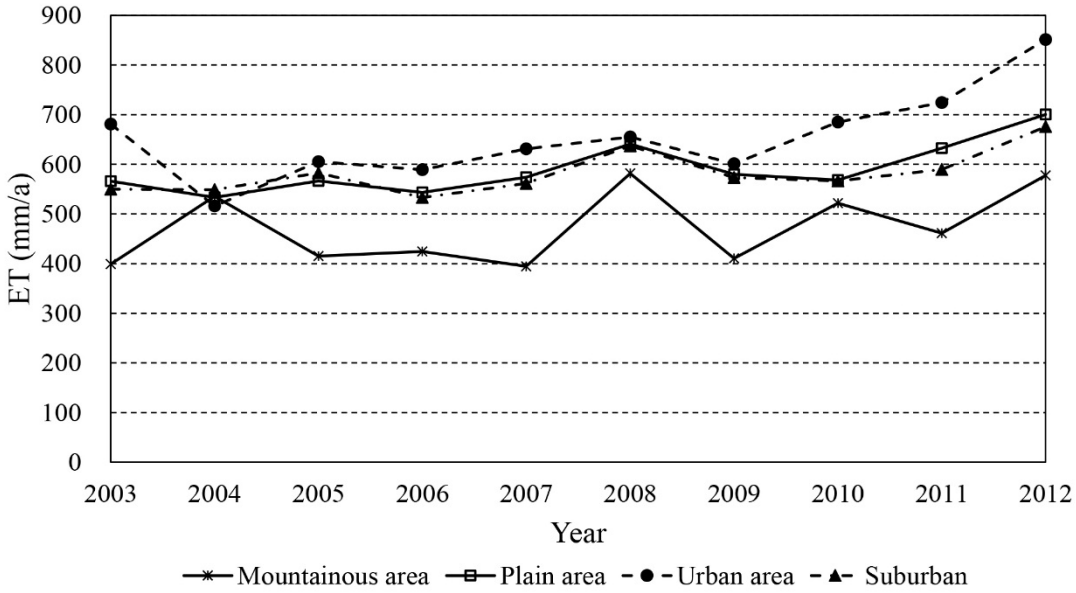

365

Figure 4. Time series of ET estimation from water balance method in subareas of Beijing during 2003-2012.

366

367 **Table 4** Annual precipitation and ET estimation using SEBS, SEBS-Urban and
368 water balance method (mm).

Year		2003	2004	2005	2006	2007	2008	2009	2010	2011	2012	Average
Entire area	Water balance	453	534	474	471	472	603	476	538	521	625	517
	SEBS	564	510	541	490	461	549	500	523	551	581	527
	SEBS-Urban	592	546	574	529	506	595	543	586	607	643	572
	P	453	539	468	448	449	638	448	524	552	708	523
Mountainous area	Water balance	399	536	415	424	395	582	410	522	461	578	472
	SEBS	581	540	561	513	478	566	509	545	578	587	546
	SEBS-Urban	582	542	563	516	481	568	511	550	581	593	549
	P_m	425	558	442	434	407	648	419	542	492	652	502
Plain area	Water balance	566	533	567	544	574	641	580	568	632	700	591
	SEBS	538	462	508	452	433	523	485	488	507	571	497
	SEBS-Urban	607	553	590	550	547	637	596	644	650	725	610
	P_p	525	510	510	470	495	625	494	501	665	796	559
Urban area	Water balance	681	516	605	589	631	655	601	685	724	851	654
	SEBS	395	270	328	305	297	372	301	329	361	518	348
	SEBS-Urban	665	537	591	607	613	679	594	658	698	882	652
	P_u	634	602	450	505	558	680	496	622	743	911	620
Suburban area	Water balance	550	549	582	533	561	637	573	566	589	676	582
	SEBS	569	504	547	484	463	555	524	523	538	582	529
	SEBS-Urban	593	556	589	536	532	627	595	640	638	691	600
	P_s	510	501	548	462	481	611	493	498	634	780	552

4.2 ET estimated by original SEBS

The annual ET values estimated from original SEBS are listed in **Table 4**. It represents a contrary results from water balance method that mountainous area has the highest average ET of 546 mm, while urban area has the lowest average ET of 348 mm. In this study, 2003, 2006, 2009 and 2012 had been selected as the typical years for comparison. The spatial variability of annual ET was significant large over the entire Beijing and the lowest ET was found in urban area (see **Figure 5**).

4.3 ET estimated by SEBS-Urban

The annual ET calculated using SEBS-Urban are listed in **Table 4**. It can be seen that annual ET in urban area was the highest among all subareas (652 mm), while the lowest in mountainous area (549 mm), which was coincident with the result from water balance method. ET spatial patterns vary dramatically over the entire Beijing as illustrated by **Figure 5**. It can be observed that higher ET values across the study region were yielded in urban area, and an increasingly trend was also observed from 2003 to 2012.

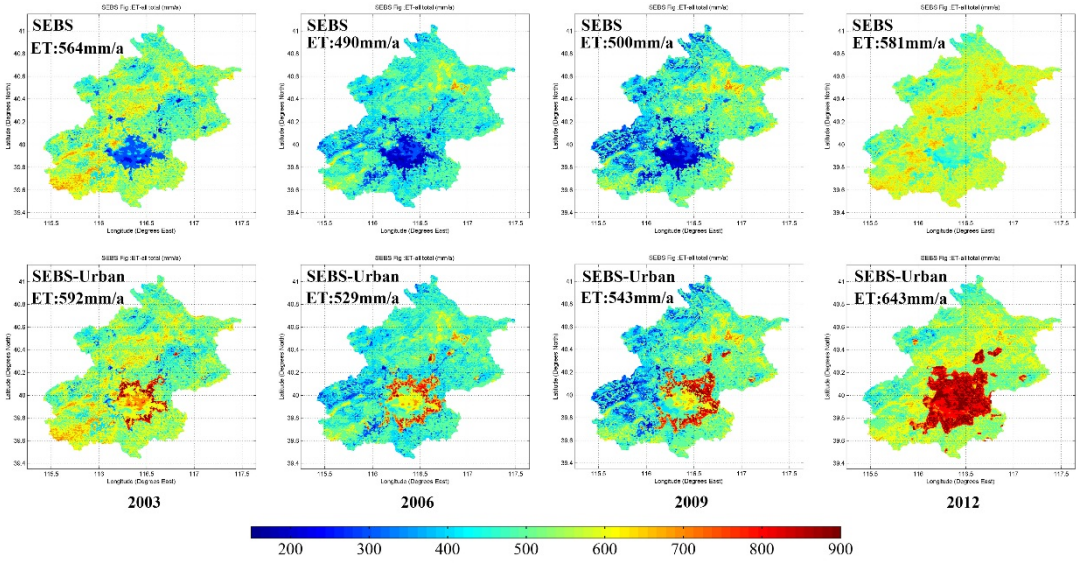

Figure 5. Annual values and spatial distribution of ET estimation using SEBS and SEBS-Urban in the typical years.

4.4 Comparison of ET estimated by different methods

The relationships between ET estimation from water balance method and remotely-sensed models in subareas of Beijing from 2003 to 2012 are demonstrated in **Figure 6**, and the corresponding ET values are given in **Table 4**. It should be noted that averaged annual ET in urban area was the highest among all subareas using water balance method (654 mm) and SEBE-Urban (652 mm). The anthropogenic heat-impacted areas were extracted from the night-light maps with a numeric value greater than 52, and the variation is demonstrated in **Figure 7** and **Figure 8**. From **Figure 7**, it can be seen that in 2003, the extreme values of anthropogenic heat were mainly concentrated in Xicheng Distict, Dongcheng Distict, while partially occurred in Haidian Distict and Chaoyang Distict. The impact of anthropogenic heat gradually intensified from 2003 to 2012 (see **Figure 8**). By 2012, the concentrations of anthropogenic heat extended to the entire urban area as well as some surrounding suburban regions, showing a great expansion in the past decade (see **Figure 7**). In urban area, the existence

of water bodies (e.g. artificial lakes and moats) and constant irrigation for gardens, lawns and other greenbelts provide sufficient water for ET purposes. On the other hand, anthropogenic heat emission from human metabolism, industrial sector, vehicles and buildings contribute greatly to the surface energy budget (Allen et al., 2011; McCarthy et al., 2010; Sailor, 2011). These two reasons above can result in a wet-limit condition (energy at limiting cases), which could be a main ET additional part compared to suburban area. Moreover, domestic water use in the buildings could also be a main additional part of ET. The teeming industrial hubs, vehicle exhaust, and densely populated make the heart of Beijing city particularly concentrated with anthropogenic heat. Therefore, the regions with high value of anthropogenic heat could be the main ET additional parts compared to suburban area. It can also be observed that ET values estimated by SEBS-Urban showed an agreement with water balance-based estimates in urban area, suburban area and plain area, where ET values were underestimated by SEBS (see **Figure 6c, 6d, 6e**). Specifically, compared to water balance method, a very high correlation coefficient (0.97) as well as small Bias (-0.24%) were showed in urban area by SEBS-Urban, while a sharp underestimation in ET values from SEBS was observed in urban area (-46.84%). In addition, the results from SEBS and SEBS-Urban were approximately equal in mountainous area (see **Figure 6b**), which were in accord with the fact that the anthropogenic heat-free areas distribute mostly in mountainous area. This provides an insight on how greatly anthropogenic heat impact on ET. Therefore, this heat should be included in the urban surface energy budget for an accurate estimation of ET in the highly urbanized areas.

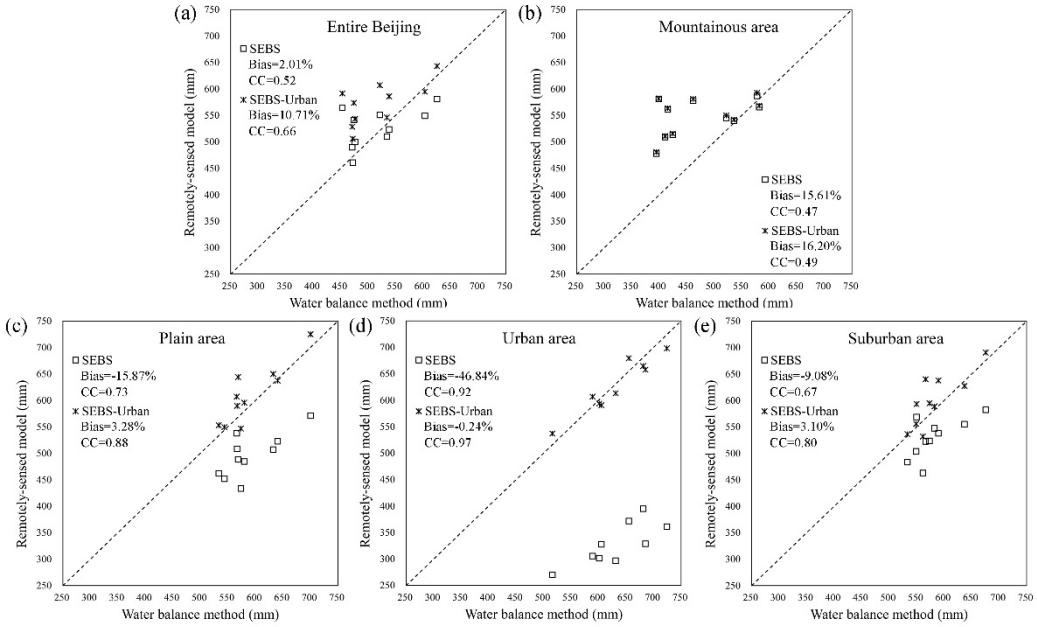

Figure 6. Relationships between ET estimation based on water balance method and remotely-sensed models in subareas of Beijing during 2003-2012.

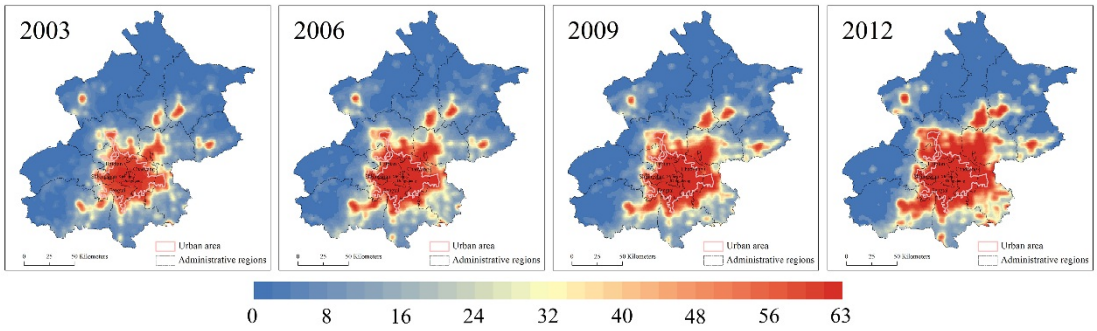

Figure 7. The distribution of anthropogenic heat-impacted areas in Beijing in the typical years.

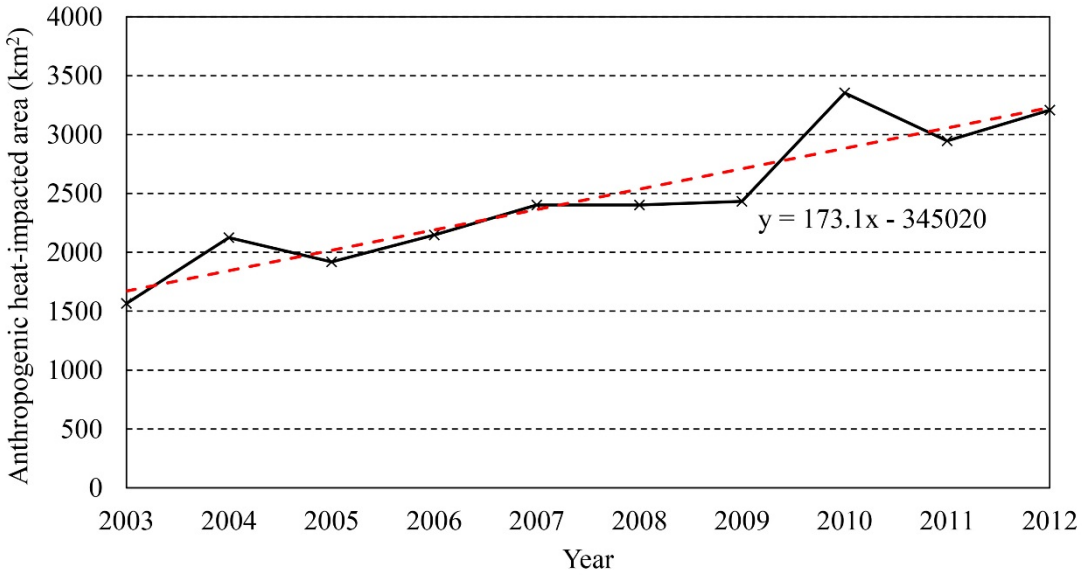

Figure 8. The evolution of anthropogenic heat-impacted areas in Beijing from 2003 to 2012.

4.5 Uncertainty analysis

It should be noted that there were some uncertainties existed in ET estimation. As for water balance model, the groundwater inflow was assumed to be equal to groundwater outflow in Beijing city due to the lack of measured data, which would produce uncertainty in ET estimation. Besides, uncertainties could also come from the annual precipitation in subareas, which were estimated according to meterological stations and local precipitation contour map. In remote sensing-based methods, a major concern is the quality of satellite image which are greatly influenced by weather condition in the study region. The uncertainties were somehow generated from the subjective selection of the cloud-free days in the year.

Actually aerosol can contribute to additional large-scale decrease in radiation budget in the metropolises like Beijing (Charlson and Schwartz, 1992; Hansen et al., 1997; Haywood and Shine, 1995; Kushta et al., 1995; Papayannis et al., 1998). In this study, the long time scale extension was based on the ratio of estimated ET_0 and the corresponding ET_0 for the days of image available, then the actual ET for days without good quality images could be inferred. Note that aerosol played an essential role in sunshine duration, which has a great influence on net radiation, and then the ET_0. Therefore, aerosol effect was not considered in the estimation of cloud-free days ET,

but was implicitly considered in the crop coefficient method which was used to extend time series of ET. However, the extension of long-time series of ET would lead to some uncertainties if the intervals between images available were not accordance with the actual case.

5. Conclusions

In this study, water balance method, energy balance model SEBS and SEBS-Urban were used to estimate ET of Beijing from 2003 to 2012. Our results have shown that:

(1) Based on water balance method, the average ET over 2003 to 2012 was 517 mm in entire Beijing. The urban area had the highest ET value (654 mm), while the mountainous area had the lowest value (472 mm).

(2) Using SEBS model, the annual average ET in urban area was sharply underestimated with a value of 348 mm. By the modified model SEBS-Urban, annual average ET in urban area was the highest among all subareas (652 mm), while the lowest in mountainous area (549 mm), which was coincident with the result from water balance method.

(3) Time series of ET estimated by SEBS-Urban showed a good agreement with water balance method in urban area.

The results indicate that anthropogenic heat should be included in the surface energy budget for a highly urbanized area. Further study should focus on detailed analysis on the evaluation of anthropogenic heat as well as the impact of net advection.

Acknowledgements

This work was supported by the National Natural Science Foundation of China under Grant Number 51279208 and 51179083. The forcing dataset used in this study was developed by Data Assimilation and Modeling Center for Tibetan Multi-spheres, Institute of Tibetan Plateau Research, Chinese Academy of Sciences. We would like to thank Beijing Water Authority, Beijing Municipal Bureau of Statistics, NASA and NOAA for providing data freely. Also we are grateful to Prof. Zongbo Su for the assistance in SEBS programming.

References

Alexandris S, Stricevic R and Petkovic S, 2008. Comparative analysis of reference evapotranspiration from the surface of rainfed grass in central Serbia, calculated by six empirical methods against the Penman-Monteith formula. European Water, 21(22): 17-28.

Allen L, Lindberg F and Grimmond C, 2011. Global to city scale urban anthropogenic heat flux: model and variability. Int J Climatol, 31(13): 1990-2005.

Allen R G, Morse A, Tasumi M, Bastiaanssen W, Kramber W and Anderson H, 2001. Evapotranspiration from Landsat (SEBAL) for water rights management and compliance with multi-state water compacts. In Geoscience and Remote Sensing Symposium, IGARSS'01. IEEE 2001 International, Vol. 2, pp. 830-833.

Allen R G, 2000. Using the FAO-56 dual crop coefficient method over an irrigated region as part of an evapotranspiration intercomparison study. J Hydrol, 229(1): 27-41.

Allen R G, Pereira L S, Raes D and Smith M, 1998. Crop evapotranspiration-Guidelines for computing crop water requirements-FAO Irrigation and drainage paper 56. FAO, Rome, 300(9): D05109.

Allen R G, Tasumi M and Trezza R, 2007. Satellite-based energy balance for mapping evapotranspiration with internalized calibration (METRIC)—Model. Journal of

Irrigation and Drainage Engineering, 133(4): 380-394.
Alley W M, 1984. On the treatment of evapotranspiration, soil moisture accounting, and aquifer recharge in monthly water balance models. Water Resour Res, 20(8): 1137-1149.
Bai X and Imura H, 2001. Towards sustainable urban water resource management: a case study in Tianjin, China. Sustainable Development, 9(1): 24-35.
Bastiaanssen W, Menenti M, Feddes R A and Holtslag A, 1998. A remote sensing surface energy balance algorithm for land (SEBAL). 1. Formulation. J Hydrol, 212: 198-212.
Beljaars A and Holtslag A, 1991. Flux parameterization over land surfaces for atmospheric models. J Appl Meteorol, 30(3): 327-341.
Bratman G N, Daily G C, Levy B J and Gross J J, 2015. The benefits of nature experience: Improved affect and cognition. Landscape and Urban Planning, 138: 41-50.
Brutsaert W, 1982. Evaporation into the Atmosphere-Theory, History and Application. D. Reidel pub. Comp, Dordrecht-Boston-London.
Brutsaert W, 1999. Aspects of bulk atmospheric boundary layer similarity under free‐convective conditions. Rev Geophys, 37(4): 439-451.
Charlson R J, Schwartz S E, 1992. Climate forcing by anthropogenic aerosols. Science, 255(5043): 423-230.
Che W R, 2008. Annual Water Utilization Estimation of main Trees, Shrubs and Lawn Grass Species of Greenland in Beijing. Master's Dissertation. Beijing: Beijing Forestry University (in Chinese).
DiGiovanni K, Montalto F, Gaffin S and Rosenzweig C, 2012. Applicability of classical predictive equations for the estimation of evapotranspiration from urban green spaces: green roof results. Journal of Hydrologic Engineering, 18(1): 99-107.
Du L X and Xing S H, 2009. Relationship between Spatial Distribution Pattern of Shrub Community and Environmental Factors in Badaling of Beijing. Acta Botanica Boreali-Occidentalia Sinica, 29(3): 601-607 (in Chinese).
Flanner M G, 2009. Integrating anthropogenic heat flux with global climate models. Geophys Res Lett, 36(2).
Gillies R R and Carlson T N, 1995. Thermal remote sensing of surface soil water content with partial vegetation cover for incorporation into climate models. J Appl Meteorol, 34(4): 745-756.
Granier A, Bréda N, Biron P and Villette S, 1999. A lumped water balance model to evaluate duration and intensity of drought constraints in forest stands. Ecol Model, 116(2): 269-283.
Grimmond C S B and Oke T R, 1991. An evapotranspiration‐interception model for urban areas. Water Resour Res, 27(7): 1739-1755.
Hansen J, Sato M, Ruedy R, 1997. Radiative forcing and climate response. J Geophys Res: Atmospheres, 102(D6): 6831-6864.
Haywood J M, Shine K P, 1995. The effect of anthropogenic sulfate and soot aerosol on the clear sky planetary radiation budget. Geophys Res Lett, 22(5): 603-606.
He G J, Chen G, He X Y, Wang, W and Liu D S, 2001. Extracting Buildings Distribution Information of Different Heights in a City from the Shadows in a Panchromatic SPOT Image. Journal of Image and Graphics, 6(5): 425-428 (in Chinese).
He J, Yang K. China Meteorological Forcing Dataset. Cold and Arid Regions Science Data Center at Lanzhou, 2011. doi:10.3972/westdc.002.2014.db
Heilig G K, 2012. World urbanization prospects: the 2011 revision. United Nations, Department of Economic and Social Affairs (DESA), Population Division,

Population Estimates and Projections Section, New York.
Ichinose T, Shimodozono K and Hanaki K, 1999. Impact of anthropogenic heat on urban climate in Tokyo. Atmos Environ, 33(24): 3897-3909.
Iglesias A, Garrote L, Flores F and Moneo M, 2007. Challenges to manage the risk of water scarcity and climate change in the Mediterranean. Water Resources Management, 21(5): 775-788.
Jia L, Xi G, Liu S, Huang C, Yan Y, and Liu G, 2009. Regional estimation of daily to annual regional evapotranspiration with MODIS data in the Yellow River Delta wetland. Hydrol Earth Syst Sci, 13(10): 1775-1787.
Jiang Y, 2009. China's water scarcity. J Environ Manage, 90(11): 3185-3196.
Kłysik K, 1996. Spatial and seasonal distribution of anthropogenic heat emissions in Lodz, Poland. Atmos Environ, 30(20): 3397-3404.
Kushta J, Kallos G, Astitha M, Solomos S, Spyrou C, Mitsakou C, and Lelieveld J, 2014. Impact of natural aerosols on atmospheric radiation and consequent feedbacks with the meteorological and photochemical state of the atmosphere. J Geophys Res: Atmospheres, 119(3): 1463-1491.
Li S S and Yang S N, 2015. Changes of extreme temperature events in Beijing during 1960-2014. Science Geographica Sinica, 35(12): 1640-1647 (in Chinese).
Liang S, 2001. Narrowband to broadband conversions of land surface albedo I: Algorithms. Remote Sens Environ, 76(2): 213-238.
Long D and Singh V P, 2010. Integration of the GG model with SEBAL to produce time series of evapotranspiration of high spatial resolution at watershed scales. J Geophys Res: Atmospheres, 115(D21).
McCarthy M P, Best M J and Betts R A, 2010. Climate change in cities due to global warming and urban effects. Geophys Res Lett, 37(9).
McMahon T A, Peel M C, Lowe L, Srikanthan R and McVicar T R, 2013. Estimating actual, potential, reference crop and pan evaporation using standard meteorological data: a pragmatic synthesis. Hydrol Earth Syst Sci, 17(4): 1331-1363.
Morse A, Tasumi M, Allen R G and Kramber W J, 2000. Application of the SEBAL methodology for estimating consumptive use of water and streamflow depletion in the Bear River basin of Idaho through remote sensing. Idaho Department of Water Resources-University of Idaho.
Nie W S, Sun T and Ni G H, 2014. Spatiotemporal characteristics of anthropogenic heat in an urban environment: a case study of Tsinghua campus. Build Environ, 82: 675-686.
Oke T R, 2002. Boundary layer climates. Routledge.
Palmroth S, Katul G G, Hui D, McCarthy H R, Jackson R B, and Oren R, 2010. Estimation of long‐term basin scale evapotranspiration from streamflow time series. Water Resour Res, 46(10).
Papayannis A, Balis D, Bais A, Van der Bergh H, Calpini B, Durieux E, Fiorani L, Jaquet L, Ziomas I, and Zerefos C S, 1998. Role of urban and suburban aerosols on solar UV radiation over Athens, Greece. Atmos Environ, 32(12): 2193-2201.
Paul M J and Meyer J L, 2008. Streams in the urban landscape. Springer, pp. 207-231.
Penman H L, 1948. Natural evaporation from open water, bare soil and grass. The Royal Society, pp. 120-145.
Pigeon G, Legain D, Durand P and Masson V, 2007. Anthropogenic heat release in an old European agglomeration (Toulouse, France). Int J Climatol, 27(14): 1969-1981.
Priestley C and Taylor R J, 1972. On the assessment of surface heat flux and evaporation

595 using large-scale parameters. Mon Weather Rev, 100(2): 81-92.
596 Roerink G J, Su Z and Menenti M, 2000. S-SEBI: A simple remote sensing algorithm
597 to estimate the surface energy balance. Phys Chem Earth, Part B: Hydrology,
598 Oceans and Atmosphere, 25(2): 147-157.
599 Sailor D J, 2011. A review of methods for estimating anthropogenic heat and moisture
600 emissions in the urban environment. Int J Climatol, 31(2): 189-199.
601 Sailor D J and Lu L, 2004. A top–down methodology for developing diurnal and
602 seasonal anthropogenic heating profiles for urban areas. Atmos Environ, 38(17):
603 2737-2748.
604 Senay G B, Leake S, Nagler P L, Artan G, Dickinson J, Cordova J T, and Glenn E P,
605 2011. Estimating basin scale evapotranspiration (ET) by water balance and remote
606 sensing methods. Hydrol Process, 25(26): 4037-4049.
607 Shi Y F, Wang X Q, Sun Z H, Chen Y Z and Fu Q K, 2015. Urban Building Heights
608 Estimation from the Shadow Information on ZY-3 Images. Journal of Geo-
609 information Science, 17(2): 236-243 (in Chinese).
610 Shu S, Yu B L, Wu J P and Liu H X, 2011. Methods for deriving urban built up area
611 using night light data: Assessment and application. Remote Sens Technol Appl,
612 26: 169-176 (in Chinese).
613 Song Z W, Zhang H L, Huang J and Chen F, 2009. Characters of Water Requirement
614 for Main Crops and Field Water Balance in Beijing Region. Research of
615 Agricultural Modernization, 30(4): 461-465 (in Chinese).
616 Su Z, 2002. The Surface Energy Balance System (SEBS) for estimation of turbulent
617 heat fluxes. Hydrology and Earth System Sciences Discussions, 6(1): 85-100.
618 Su Z, Schmugge T, Kustas W P and Massman W J, 2001. An evaluation of two models
619 for estimation of the roughness height for heat transfer between the land surface
620 and the atmosphere. J Appl Meteorol, 40(11): 1933-1951.
621 Sugita M and Brutsaert W, 1991. Daily evaporation over a region from lower boundary
622 layer profiles measured with radiosondes. Water Resour Res, 27(5): 747-752.
623 Sumner D M and Jacobs J M, 2005. Utility of Penman–Monteith, Priestley–Taylor,
624 reference evapotranspiration, and pan evaporation methods to estimate pasture
625 evapotranspiration. J Hydrol, 308(1): 81-104.
626 Tam B Y, Gough W A and Mohsin T, 2015. The impact of urbanization and the urban
627 heat island effect on day to day temperature variation. Urban Climate, 12: 1-10.
628 Tong H, Liu H Z, Sang J G and Hu F, 2004. The Impact of Urban Anthropogenic Heat
629 on Beijing Heat Environment. Climatic and Environmental Research, 9(3): 409-
630 421 (in Chinese).
631 Van den Hurk B and Holtslag A, 1997. On the bulk parameterization of surface fluxes
632 for various conditions and parameter ranges. Bound-Layer Meteor, 82(1): 119-133.
633 Wang Y and Wang H, 2005. Sustainable use of water resources in agriculture in Beijing:
634 problems and countermeasures. Water Policy, 7(4): 345-357.
635 Xu C and Singh V P, 2005. Evaluation of three complementary relationship
636 evapotranspiration models by water balance approach to estimate actual regional
637 evapotranspiration in different climatic regions. J Hydrol, 308(1): 105-121.
638 Xu M Y, Li Y Q, Wang K, Cao Y F, Yu H L, Li X F, Li L S, Jing F J, Li J X and Xie F,
639 2009. Spatial distribution and dynamic characteristics of the grassland vegetation
640 in Hebei. Acta Prataculturae Sinica, 18(6): 1-11 (in Chinese).
641 Yang J, Wang Z H, Chen F, Miao S, Tewari M, Voogt J A and Myint S, 2015. Enhancing
642 Hydrologic Modelling in the Coupled Weather Research and Forecasting–Urban
643 Modelling System. Bound-Layer Meteor, 155(1): 87-109.
644 Yang L, Niyogi D, Tewari M, Aliaga D, Chen F, Tian F Q and Ni G H, 2016. Contrasting

impacts of urban forms on the future thermal environment: example of Beijing metropolitan area. Environ Res Lett, 11(3): 034018.
You H L, Ren G Y, Liu W D, 2012. Precipitation changes over the beijing area during 1961-2010. Desert and Oasis Meteorology, 6(4): 13-20 (in Chinese).
Zhang C L, Chen F, Miao S G, Li Q C, Xia X A and Xuan C Y, 2009. Impacts of urban expansion and future green planting on summer precipitation in the Beijing metropolitan area. J Geophys Res: Atmospheres, 114(D2).
Zhang L J, Sun C Z, Xin X B and Kong Q Y, 2014. Allometric relationship between height and diameter at breast height of different stand in Beijing Jiulong mountain. Journal of Central South University of Forestry & Technology, 34(12): 66-70 (in Chinese).
Zhang X W, 2011. Studies on the canopy structrue of plant communities in some Beijing greenbelt. Master's Dissertation. Beijing: Beijing Forestry University (in Chinese).
Zheng W W, 2012. Inversion of evapotranspiration on urban land surface based on remote sensing data. Doctoral Dissertation. Changsha: Central South University (in Chinese).
Zhong S, Qian Y, Zhao C, Leung R and Yang X Q, 2015. A case study of urbanization impact on summer precipitation in the Greater Beijing Metropolitan Area: Urban heat island versus aerosol effects. J Geophys Res: Atmospheres, 120(20).